



# HHS Public Access

Author manuscript

*Res Rep Nucl Med.* Author manuscript; available in PMC 2016 October 14.

Published in final edited form as:

*Res Rep Nucl Med.* 2015 ; 5: 19–32. doi:10.2147/RRNM.S81742.

## Double agents and secret agents: the emerging fields of exogenous chemical exchange saturation transfer and T<sub>2</sub>-exchange magnetic resonance imaging contrast agents for molecular imaging

Iman Daryaei<sup>1</sup> and Mark D Pagel<sup>1,2,3,4</sup>

<sup>1</sup>Department of Chemistry and Biochemistry, University of Arizona, Tucson, AZ, USA

<sup>2</sup>Department of Biomedical engineering, University of Arizona, Tucson, AZ, USA

<sup>3</sup>Department of Medical Imaging, University of Arizona, Tucson, AZ, USA

<sup>4</sup>The University of Arizona Cancer Center, Tucson, AZ, USA

### Abstract

Two relatively new types of exogenous magnetic resonance imaging contrast agents may provide greater impact for molecular imaging by providing greater specificity for detecting molecular imaging biomarkers. Exogenous chemical exchange saturation transfer (CEST) agents rely on the selective saturation of the magnetization of a proton on an agent, followed by chemical exchange of a proton from the agent to water. The selective detection of a biomarker-responsive CEST signal and an unresponsive CEST signal, followed by the ratiometric comparison of these signals, can improve biomarker specificity. We refer to this improvement as a “double-agent” approach to molecular imaging. Exogenous T<sub>2</sub>-exchange agents also rely on chemical exchange of protons between the agent and water, especially with an intermediate rate that lies between the slow exchange rates of CEST agents and the fast exchange rates of traditional T<sub>1</sub> and T<sub>2</sub> agents. Because of this intermediate exchange rate, these agents have been relatively unknown and have acted as “secret agents” in the contrast agent research field. This review exposes these secret agents and describes the merits of double agents through examples of exogenous agents that detect enzyme activity, nucleic acids and gene expression, metabolites, ions, redox state, temperature, and pH. Future directions are also provided for improving both types of contrast agents for improved molecular imaging and clinical translation. Therefore, this review provides an overview of two new types of exogenous contrast agents that are becoming useful tools within the armamentarium of molecular imaging.

---

This work is published by Dove Medical Press Limited, and licensed under Creative Commons Attribution – Non Commercial (unported, v3.0) License. The full terms of the License are available at <http://creativecommons.org/licenses/by-nc/3.0/>. Non-commercial uses of the work are permitted without any further permission from Dove Medical Press Limited, provided the work is properly attributed. Permissions beyond the scope of the License are administered by Dove Medical Press Limited. Information on how to request permission may be found at: <http://www.dovepress.com/permissions.php>

Correspondence: Mark D Pagel, The University of Arizona Cancer Center, 1501 North Campbell Avenue, Tucson, AZ 85724, USA, Tel +1 520 404 7049, Fax +1 520 626 0395, [mpagel@u.arizona.edu](mailto:mpagel@u.arizona.edu).

### Disclosure

The authors report no conflicts of interest in this work.

## Keywords

CEST;  $T_{2ex}$ ;  $T_2$  relaxation; responsive agents; exchange rate

---

## Introduction

Magnetic resonance imaging (MRI) has become a popular tool for anatomical imaging of organs and pathological tissues.<sup>1</sup> The development of exogenous MRI contrast agents has greatly contributed to clinical MRI since the first in vivo application of contrast agents was introduced 37 years ago.<sup>2</sup>  $T_1$  MRI contrast agents can brighten the image contrast of tissues with the agent, which has led to their widespread use for clinical diagnoses.  $T_2^*$  MRI contrast agents darken the image of the tissues with the agent, which also has good utility for some clinical diagnoses. However, many physicochemical characteristics can affect the image contrast of tissues with a  $T_1$  or  $T_2^*$  contrast agent, which limits quantitative analyses with these agents. In particular, a change in image contrast can be difficult to assign to the presence of a biomarker in a tissue because other characteristics such as the concentration of the agent in tissue can also change image contrast. Therefore,  $T_1$  and  $T_2^*$  MRI contrast agents have been difficult to apply to molecular imaging.

Two new types of exogenous contrast agents have been developed to improve molecular imaging with MRI. Chemical exchange saturation transfer (CEST) contrast agents exploit the MR frequency (chemical shift) of an agent to selectively generate contrast in a MR image. Importantly, two CEST effects on a single agent or two similar agents can be detected, and the ratio of these two CEST effects can improve the quantitative evaluations of molecular imaging in a concentration-independent manner. In this review, we refer to these agents as “double agents” to emphasize the importance of this advantage of CEST agents.<sup>3</sup> In addition, many endogenous biomolecules can generate CEST effects, such as metabolites and peptides, produced through transcription and translation of artificial genes. Our review does not extensively discuss endogenous CEST agents, which are already described in other excellent reviews.

A contrast agent based on  $T_2$  exchange ( $T_{2ex}$ ) can change the  $T_2$ -weighted MRI contrast without also changing  $T_1$ -weighted MRI contrast. The ratio of  $T_2/T_1$  has potential to improve the quantitative evaluations of molecular imaging in a concentration-independent manner. The  $T_{2ex}$  mechanism requires a chemical exchange rate in a moderately fast regime that has often been unrecognized until recently. For this reason, we refer to these agents as “secret agents” to emphasize that  $T_{2ex}$  agents should no longer be secret and should be recognized for their importance to molecular imaging with MRI.

## Exogenous CEST MRI contrast agents

CEST MRI contrast agents have one or more exchangeable protons that can be part of the covalent structure of the agent or a proton on a metal-bound water in the inner sphere of the contrast agent. When the magnetization (MRI frequency) of the exchangeable proton is saturated with radiofrequency pulses (Figure 1A), then the net magnetic properties of these protons become “saturated” and lose their detectable MRI signal. Upon exchange of these

protons with the bulk water protons (Figure 1B), this saturation is transferred to the bulk water (Figure 1C) and the MR image of the bulk water becomes darker. Repeating this process for a range of radiofrequencies can be used to generate a Z-spectrum (Figure 1D), also known as a CEST spectrum (Figure 1E). The center of the Z-spectrum represents the direct saturation of bulk water and is defined as zero saturation frequency in the Z-spectrum.<sup>4</sup>

The chemical exchange rate of the proton from the agent to bulk water is critical for generating CEST MRI contrast for molecular imaging. The exchange rate must be slower than the chemical shift difference between the agent and bulk water, so that the exchangeable proton exists at the chemical shift of the agent for a sufficient time to be saturated by the radiofrequency pulse. However, faster chemical exchange rates generate more transfer of saturation per unit time, which increases CEST MRI contrast. Therefore, agents with chemical exchange rates of 100–30,000 Hz are typically regarded to be CEST MRI contrast agents. Paramagnetic CEST (paraCEST) agents have larger chemical shifts and typically have chemical exchange rates that are >1,000 Hz. Diamagnetic CEST (diaCEST) agents have chemical shifts within 12 ppm of bulk water and thus have exchange rates that are typically <2,000 Hz (although a few diaCEST agents have exchange rates that exceed 2,000 Hz).<sup>5</sup> Furthermore, the chemical exchange rate can be altered after the agent interacts with a biomarker. As described by examples listed below, the quantitative measurement of changes in chemical exchange rates of CEST agents, or the changes in CEST signals that result from changes in exchange rates, can exquisitely detect the presence of the biomarker.

### CEST agents that detect enzyme activities

Many CEST agents have been developed that detect enzyme activity. One or more covalent bonds of the agent can be cleaved or created by the enzyme, which can drastically affect the chemical exchange rate of the labile proton of the agent. This irreversible change in the agent facilitates the accumulation of a high concentration of altered agent. Therefore, a low concentration of an enzyme with fast catalytic activity can be detected with this imaging approach. A second CEST agent, or a second exchangeable proton on the same agent, can be designed to have a unique chemical shift for selective CEST detection, and therefore, creates a double-agent approach. This second CEST effect can also be designed to be unaffected by the enzyme and therefore, serve as an unresponsive “control” agent to improve the quantitative detection of enzyme activity.

One of the first examples of an enzyme-responsive paraCEST agent is a Tm(III) macrocyclic chelate conjugated to the C-terminal end of a peptide, which serves as a substrate for the caspase-3 protease enzyme (Figure 2A).<sup>6</sup> Cleavage of the peptide from the Tm(III) chelate converts an amide group to an amine group. This conversion changes the chemical shift of the CEST effect from –51 ppm to +8 ppm and also increases the chemical exchange rate. A Yb(III) chelate without a peptide was not catalyzed by caspase-3, which served as the double agent for comparison to the responsive CEST agent. This double-agent approach improved the quantification of enzyme activity. During these studies, the caspase-3-responsive agent was used to measure the activity of 3.44 nM of caspase-3 enzyme, which

confirmed that high catalytic enzyme activity can be exploited to detect sufficient concentrations of the agent.

This platform technology has enabled the detection of other enzymes, such as cathepsin D and urokinase plasminogen activator, simply by changing the conjugated peptide sequence to peptides specific to each enzyme (Figure 2B and C).<sup>7,8</sup> A second CEST agent was used as the double agent to improve detection of the enzyme. CEST MRI was also employed to monitor the formation of a covalent bond when a paraCEST agent was conjugated to the arginine side chains of a protein by the enzyme transglutaminase (Figure 2D).<sup>9</sup> This conjugation caused an appearance of a CEST signal at  $-9.2$  ppm from a newly formed amide group between the agent and an arginine side chain. In addition, the CEST signal at  $+4.6$  ppm from the arginine side chains of the protein decreased after being conjugated to the agent. Thus, these two CEST effects could be exploited as a double agent to improve the detection of the enzyme.

ParaCEST agents have also been developed in which the macrocyclic chelate is separated from an enzyme-sensitive substrate ligand with a spontaneously disassembling linker. This technology allows the substrate ligand to be easily changed to detect other enzymes, without affecting the macrocyclic chelate that generates the CEST effect. For example, a galactose sugar ligand of a Yb(III) macrocyclic chelate can be cleaved by a  $\beta$ -galactosidase enzyme, which causes spontaneous disassembly of a benzyloxycarbamate linker. This spontaneous reaction converts an amide group to an amine group on the chelate, which changes the CEST signal from  $-16.7$  ppm to  $-20.5$  ppm (Figure 2E).<sup>10</sup> As another example, an ester ligand of a CEST agent can be cleaved by an esterase enzyme, causing a spontaneous intermolecular lactonization of a linker, which releases the ligand and linker from a Yb(III) chelate (Figure 2F).<sup>11</sup> This multistep process converts an amide group to an amine group on the Yb(III) chelate, creating a new CEST signal at  $+9$  ppm due to the proximity of the amine to the Yb(III) ion. This agent has another amide group that is unaffected by the enzyme-triggered series of reactions, which was used as an internal control to improve the quantification of this double agent.

DiaCEST agents have also been used to detect enzyme activities. For example, cytosine and its derivatives can generate CEST effects. These CEST effects are lost when cytosine deaminase catalyzes covalent changes to these diaCEST agents (Figure 3A).<sup>12</sup> Similarly, 3,5-difluorobenzoyl-L-glutamate loses its CEST signal after being catalyzed by carboxypeptidase G2.<sup>13</sup> For both of these cases, only one CEST signal was monitored from the diaCEST agent and a double-agent approach was not used, which has limited the in vivo translation of these agents.

### CEST agents that detect nucleic acids

ParaCEST agents have been used to detect DNA. A polymeric Eu(III) chelate can interact with DNA of salmon testes, which reduces the CEST amplitude by  $\sim 33\%$  due to a change in chemical exchange rate (Figure 3B).<sup>14</sup> This interaction did not change the chemical shift of the CEST effect of this agent. A dimeric Nd(III) macrocyclic chelate has been shown to interact with a DNA hairpin, causing a  $\sim 15\%$  increase in the CEST signal without also causing a change in the  $12$  ppm chemical shift (Figure 3C).<sup>15</sup> However, the detection of

nucleic acids through their direct interaction with paraCEST MRI contrast agents is hampered by the poor detection sensitivity of CEST MRI and the low concentration of most nucleic acids within in vivo systems. This problem is especially concerning for the detection of DNA, which exists at very low concentration in vivo and is typically protected by membrane bilayers of the cell and nucleus. Therefore, these examples of CEST detection of nucleic acids provide an interesting proof-of-concept but may be difficult to optimize for practical imaging applications. Furthermore, these examples involve only one CEST effect and do not exploit a double-agent approach, which limits their ability to provide quantitative imaging results.

Although the direct detection of nucleic acids is a daunting challenge, the detection of genetic activity is an easier task. Genes that encode for long polylysine or polyarginine peptides have been transfected into cells that have then be implanted in rodent models.<sup>16–18</sup> The in vivo transcription and translation of these genes produce these long peptides, which have amide, amine, and guanidinium groups that can act as diaCEST agents. Variations of homopeptides, protamine sulfate, and green fluorescent protein have also been developed and used as reporter genes during in vitro studies.<sup>19–21</sup> A gene for one of these peptides can be tied to other genes of interest for cotranscription and cotranslation, effectively using the diaCEST peptide as a “reporter gene” to report on the activity of another gene of interest. Unfortunately, recent studies have shown that biological conditions can modulate the CEST effects of some of these peptides, such as phosphorylation, acidosis, and binding to DNA and other proteins.<sup>22</sup> A double-agent approach has potential to account for these confounding biological conditions that may compromise the assessment of the CEST reporter genes, but this approach has not yet been applied to improve evaluations of gene expressions.

### CEST agents that detect metabolites

Metabolites can often exist within in vivo systems at high concentrations >1 mM, and therefore, can be good candidates to generate sufficient sensitivity for detection via CEST MRI contrast agents. A variety of metabolites can be detected with paraCEST agents, including glucose, lactate, methyl phosphate, and nitric oxide. A Eu(III) chelate with phenyl boronate ligands can bind to glucose at a 1:1 ratio, causing a decrease in the chemical exchange rate of the water molecule that is bound to the agent, which causes a ~38% decrease in CEST signal at 50 ppm (Figure 3D).<sup>23</sup> As another example, the interaction between a lactate molecule and a Yb(III) macrocycle chelate causes a change in chemical shift from -29.1 ppm to -15.5 ppm (Figure 3E).<sup>24</sup> Similarly, a Eu(III) macrocyclic chelate with a pendant hydroxyl group was used to detect methyl phosphate (Figure 3F) by monitoring a change in chemical shift from 6 ppm to 8 ppm after reacting with the metabolite.<sup>25</sup> The change in chemical shift of a CEST agent is independent of the agent's concentration to quantify the metabolite, and therefore, does not require a double-agent approach.

Unfortunately, these CEST agents that interact with metabolites lack specificity for detecting only the intended metabolite. As examples, the glucose-detecting CEST agent also interacts with fructose, and similarly the agent that detects methyl phosphate shows a similar change

in the chemical shift of the CEST effect when interacting with ethyl phosphate. The lactate-detecting CEST agent has affinity for many other carboxylate-containing metabolites. This inherent problem with specificity is not unexpected because many metabolites have very similar chemical structures.

Most metabolite-detecting CEST agents are reversibly responsive, so that their change in CEST characteristics can “reverse” to the original state when the metabolite dissociates from the agent. This can be problematic when attempting to detect temporally fleeting metabolites. As an alternative approach, a CEST agent has been designed to be irreversibly responsive, undergoing a permanent change in the bonding of the agent after interaction with nitric oxide (Figure 3G). This irreversibly responsive change provided the advantage of accumulating a high concentration of agent over time that is sufficient for detection with CEST MRI, even though nitric oxide was not present at a similar high concentration at any instant.<sup>26</sup> More specifically, nitric oxide caused the irreversible dimerization of the agent through an azide bridge, causing a loss of amine protons and changing the conformation of the agent, which consequently resulted in the disappearance of the CEST effects of the agent. A second CEST agent that does not interact with nitric oxide was included in these studies, and this double-agent approach was used to improve the detection of nitric oxide.

Glucose<sup>27</sup> and its derivatives<sup>28–31</sup> can generate CEST signals from the exchangeable protons of the hydroxyl groups on the sugar, and therefore, this metabolite can be directly detected with CEST MRI. Although the CEST signal is weak relative to other CEST agents, a high concentration of the sugar can be administered to generate a CEST signal that is adequate for detection. Tracking the pharmacokinetics and biodistribution of glucose, or glucose derivatives that are trapped along metabolic pathways, can be exploited to image pathological tissues with altered glucose metabolism. Glucose is an Food and Drug Administration (FDA)-approved treatment for some pathological conditions, which facilitates clinical translation of CEST MRI with glucose.<sup>32</sup> However, a double-agent approach has not been employed with sugar-based CEST MRI studies, which raises concerns that other biological conditions that affect the CEST signal from glucose may complicate the analysis of sugar concentrations from CEST MRI studies.

### CEST agents that detect ions

Our deep understanding of the interactions of metals with ligands has been a primary driving force for developing paraCEST agents that detect ions. A Eu(III) complex with pendant pyridine arms has a CEST signal that changes upon binding to Zn<sup>2+</sup> ions. The exact mechanism of this change in CEST signal is not understood but may be due to a hydroxide ion coordinated to Zn<sup>2+</sup> that causes an accelerated chemical exchange rate of the complex (Figure 4A).<sup>33</sup> A similar concept was employed to detect Ca<sup>2+</sup> ions with a Yb(III)-based paraCEST agent with pendant bis-carboxylate arms.<sup>34</sup> Chelation of Ca<sup>2+</sup> ions with the Yb<sup>3+</sup> macrocyclic chelate slowed the chemical exchange rate of protons from the amide groups on the chelate and resulted in a 60% loss in CEST signals (Figure 4B). This technology has potential applications for in vivo studies. However, the change in ion concentration in biological systems could be faster than the detection of the reversibly responsive paraCEST agents, which may compromise detection sensitivity. Also, additional research is needed to



assess the specificity of detecting the intended ion relative to other ions with similar sizes and electronic charges. A clever double-agent approach may possibly aid in improving this detection specificity, as shown by some of the other double-agent approaches listed in this review.

### CEST agents that detect redox state

The redox state of the tissue environment is an important biomarker in many pathologies such as cancer and wound healing. The noninvasive detection of such tissue environments can provide great information about dysregulation of biomolecules such as reducing agents. ParaCEST agents are very well suited for detecting redox state because the oxidation state of the paramagnetic ion is highly dependent on the environmental redox state. For example, a paramagnetic Co(II) macrocyclic chelate with three pyrazole ligands can generate a strong CEST signal (Figure 4C). When exposed to reducing agents, the oxidized Co(II) metal changes to a reduced Co(III) form that is diamagnetic, so that the paraCEST effect is lost.<sup>35</sup>

The change in redox state of a paraCEST agent's ligand can also be used to monitor changes in environmental redox status. As a seminal example, two quinolinium ligands exist in an oxidized form in a Eu(III)-based paraCEST agent (Figure 4D). These ligands can be reduced by nicotinamide adenine dinucleotide, and the change in the redox state of the ligand causes a weak CEST signal at 43 ppm to become 7.5-fold stronger and shift to 50 ppm.<sup>36</sup> As another example, the anthracene ligand of another Eu(III) macrocyclic chelate can be oxidized by singlet oxygen to produce an endoperoxide derivative (Figure 4E). This oxidation caused a 3 ppm change in the chemical shift of the CEST signal. Moreover, the specificity of this reaction was shown to be outstanding for  $^1\text{O}_2$  relative to other species such as  $\text{ONOO}^-$ ,  $\text{H}_2\text{O}_2$ ,  $^*\text{OH}$ , or  $\text{O}_2^-$ .<sup>37</sup> An advantage of these two agents is the change in chemical shifts of the CEST signals that is exploited for detection of redox state. The chemical shifts are independent of concentration of the agent, thereby improving the specificity for detecting the redox state without requiring a "dual-agent" approach.

### CEST agents that measure temperature

The changes in the chemical shift of exchangeable protons in paraCEST agents have been also investigated as a method for monitoring changes in temperature. The observed chemical shift is a time-weighted average of the chemical shift of the labile proton of a contrast agent and the chemical shift of the same proton in bulk water during the CEST experiment (a phenomenon known as MR coalescence). At higher temperature, this time-weighted average moves toward the bulk water signal due to an increase in exchange rate of the proton from the agent to water. The best example of this class of agents is a Dy(III) macrocyclic chelate that exhibits a change in chemical shift from  $-800$  ppm to  $-650$  ppm over a range of temperature from  $20^\circ\text{C}$  to  $50^\circ\text{C}$ , for an impressive change of  $6.9$  ppm/ $^\circ\text{C}$  (Figure 4F).<sup>38</sup> For comparison, other paraCEST agents based on Eu(III) and Tm(III) chelates have demonstrated much smaller  $0.1$ – $0.6$  ppm/ $^\circ\text{C}$  changes in chemical shifts (Figure 4G and 4H).<sup>39,40</sup> Importantly, relying on the chemical shift of the CEST effect does not require a double-agent approach to account for the concentration of the agent because the chemical shift is inherently independent of concentration.

## CEST agents that measure pH

The amide and amine protons in paraCEST agents exhibit base-catalyzed chemical exchange. Therefore, the CEST signals generated from these functional groups are inherently pH dependent. One of the first examples of a responsive paraCEST agent, a Yb(III) chelate, had a CEST signal amplitude that was correlated with pH between 6.0 and 7.2 units (Figure 5A).<sup>41</sup> However, the CEST amplitude is also dependent on concentration, which complicates pH measurements using this single agent with a single CEST signal. To overcome this limitation, the ratio of CEST signal amplitudes from an amide proton and metal-bound water protons of a variety of lanthanide macrocyclic chelates can be used to measure pH, while this CEST ratio is concentration independent (Figure 5B).<sup>42</sup> Similarly, the amide and amine functional groups of an asymmetric Yb(III) chelate have selectively detectable CEST effects with different pH dependencies, which can also be used in a ratiometric approach to measure pH in a concentration-independent manner (Figure 3G).<sup>43</sup> These examples once again reinforce the advantages of a double-agent approach to improve quantitative imaging.

As a twist on this theme, a Yb(III) metal chelate has been designed that can interconvert between two conformations. Each conformation can generate CEST signals at different chemical shifts. The ratio of conformations depends on pH, so that the ratio of the two CEST signal amplitudes from each conformation is correlated with pH (Figure 5C).<sup>44</sup> A related example measures pH using a ratio of two CEST signal amplitudes from a paramagnetic Co(II) chelate that interconverts between two conformations (Figure 5D).<sup>45</sup> These two examples again demonstrate the advantage of a double-agent approach to remove the effects of agent concentration from the pH measurement.

Nonmetallic diaCEST agents have also exploited the double-agent approach to measure pH. Iopamidol (Isovue™; Bracco Diagnostics, Monroe Township, NJ, USA) (Figure 5E) is a FDA-approved X-ray contrast agent that can generate two CEST signals from two unique amide protons on the agent. A ratio of these two CEST signals is linearly correlated with pH in a concentration-independent manner. A similar agent, iopromide, also generates two CEST signals that can measure pH using the same ratiometric approach (Figure 5F). These agents have been used to measure pH in tumors, kidneys, cartilage, and intervertebral disks.<sup>46–49</sup> Another clever double-agent approach has used iobitridol (Figure 5G), a similar X-ray agent, that generates two CEST signals with different amplitudes when saturated with different radio frequency powers.<sup>50</sup> The ratio of these two CEST signal amplitudes is also correlated with pH.

A newer method uses the linewidth of the peak in a CEST spectrum to measure pH.<sup>51</sup> The chemical exchange rate of an amide group becomes faster at higher pH and therefore, the CEST peak becomes broader with a faster chemical exchange rate due to MR coalescence. In addition, the chemical shift of the CEST signal also changes in response to pH due to the same MR coalescence effect. A Tm(III) macrocyclic chelate with an amide group was used to measure pH within in vivo muscle tissue based on the linewidth and chemical shift of the agent's CEST signal (Figure 5H). Monitoring changes in the chemical shift of pH-dependent phenolic arms of a contrast agent is another method that has been used to evaluate pH (Figure 5I).<sup>52</sup> Notably, the linewidth and chemical shift are independent of the agent's



concentration. Thus, pH can be accurately determined from a single CEST signal without requiring a double-agent approach.

### Future directions for CEST MRI contrast agents

Although CEST MRI is a powerful technique for molecular imaging with a wide range of applications, the low sensitivity of CEST MRI relative to other MRI techniques and most other imaging modalities has had a negative impact on translation to in vivo applications. CEST agents must accumulate within in vivo tissues at millimolar concentrations for adequate detection, which may cause toxicity issues. A variety of approaches have been tested to increase the sensitivity of paraCEST agents, including polymerization,<sup>53</sup> conjugation to dendrimers<sup>54</sup> and lipids,<sup>55</sup> and encapsulation in liposomes<sup>56</sup> and supramolecular adducts.<sup>57</sup> Similar approaches have been used to detect diaCEST agents in liposomes<sup>58</sup> and supramolecular adducts.<sup>59</sup>

The paramagnetism of lanthanide ions has been tremendously useful for expanding the range of chemical shifts of paraCEST agents, which greatly facilitates their selective detection within the background of endogenous molecules during in vivo studies. However, the toxicity of lanthanide ions after the degradation of the macrocyclic chelate is a matter of concern. In particular, nephrogenic systemic fibrosis is a debilitating or morbid condition that is caused by tissue accumulation of the gadolinium lanthanide ion.<sup>60</sup> To overcome this toxicity problem, other paramagnetic ions that are nontoxic have been incorporated in paraCEST agents. To date, nontoxic Fe(II), Co(II), and Ni(II) are good candidates to replace lanthanide metals in paraCEST agents.<sup>45,61</sup> However, only certain electronic states of these transition metals are paramagnetic, and a change in electronic state can cause the ion to lose its paramagnetic properties. Although this characteristic was successfully exploited to create a redox-sensitive paraCEST agent as described earlier, the instability of the paramagnetic state of these transition metals is generally problematic for ensuring that the agent can be used as a paraCEST agent for detecting biomarkers other than redox state. Therefore, an active area of research involves the stabilization of the paramagnetic electronic state of these transition metals in macrocyclic chelates for use as responsive paraCEST agents.

### Exogenous $T_{2ex}$ contrast agents

The  $T_2$  relaxation process in biological MR studies typically involves a through-space exchange of energy between two protons. This energy exchange causes the MR frequencies of each proton to differ, so that the individual magnetic moments evolve to have different phases, and the net sum of the magnetic moments decreases over time.  $T_2^*$  relaxation is a consequence of a similar mechanism where protons in slightly different magnetic fields have slightly different MR frequencies, leading to individual magnetic moments with different phases over time, so that the net magnetic moment decays in amplitude (Figure 6A).

$T_2^*$  MRI contrast agents consist of isolated paramagnetic ions or clusters of paramagnetic ions that cause slight changes in the magnetic field near the agent. Water molecules can temporarily bind to the  $T_2^*$  agent, or more simply diffuse through the solvation shell of the  $T_2^*$  agent, and experience these slightly different magnetic fields that cause  $T_2^*$  relaxation. Importantly, this association with the  $T_2^*$  agent can be described as chemical exchange of a

water molecule between the agent–water complex and bulk water. These chemical exchange rates can approach the fast rate of the diffusion limit (the fastest rate for chemical reactions in solution), and fast chemical exchange creates highly sensitive  $T_2^*$  agents. Unfortunately, the fleeting binding of water to the agent and the general water diffusion process are each difficult to control, which decreases the specificity of  $T_2^*$  agents for detecting specific biomolecules with molecular imaging.

For comparison, CEST MRI contrast agents exploit a physical exchange of protons between agents and water, as described in previous sections of this review. This physical chemical exchange is easier to control by incorporating specific chemical groups with labile protons into CEST agents. Physical chemical exchange can also be controlled by exploiting well-known concepts of hydrogen bonding, selecting ligands with electro-negativities that modulate the acidity of labile protons, and/or incorporating steric hindrance that inhibits the association of a water molecule with the labile proton of the agent. This control of the agent's chemical exchange properties provides more specificity for detecting many types of biomarkers. However, CEST agents must have a relatively slow chemical exchange rate, which reduces their detection sensitivity.

A new class of MRI contrast agents, known as  $T_{2ex}$  agents, has recently been rediscovered that combines the advantages of  $T_2^*$  agents and CEST agents. A physical exchange of protons occurs between a  $T_{2ex}$  agent and water.<sup>62,63</sup> The specific control of these physical chemical exchange processes improves the specificity of these agents for detecting intended biomarkers, similar to CEST agents. This physical exchange causes the MR frequency of the exchanging proton to take a time-weighted average value between the frequency of the agent and the frequency of water. Because the chemical exchange is stochastic, this time-weighted average is different for each proton experiencing chemical exchange, causing slightly different average MR frequencies for each proton. These different MR frequencies result in the decay of net coherent magnetization like  $T_2$  relaxation (Figure 6B). The chemical exchange rates of  $T_{2ex}$  agents are intermediate between  $T_2$  agents and CEST agents. Although this intermediate rate causes  $T_{2ex}$  agents to have less sensitivity than  $T_2$  agents, this intermediate rate greatly improves detection sensitivity relative to CEST agents. Interestingly, this regime of intermediate chemical exchange rates of  $T_{2ex}$  agents has not been recognized or exploited as often as other chemical exchange rates when developing MRI contrast agents. Thus, we refer to  $T_{2ex}$  agents as secret agents that deserve to be exposed and promoted.<sup>64</sup>

### **$T_{2ex}$ and the Swift–Connick equation**

The study of chemical exchange rates in MRI has greatly benefited from the modified form of equations that describe the evolution of net magnetic moments during chemical exchange, known as the Bloch–McConnell equations.<sup>65,66</sup> The effects of temperature and MR frequency on  $T_2$  relaxation in solutions containing paramagnetic ions led to modified versions of the Bloch–McConnell equations.<sup>67,68</sup> Eventually, the Swift–Connick equation was shown to agree with experimental results and has been used as the practical description of  $T_{2ex}$  relaxation (Equation 1).<sup>69</sup> The Swift–Connick equation indicates that  $T_{2ex}$  agents

should have labile protons with large chemical shifts and chemical exchange rates that are comparable to these chemical shifts (Figure 7A and B).

$$R_{2\text{ex}} = P_{\text{B}} k_{\text{ex}} \cdot \frac{R_2^2 + R_2 k_{\text{ex}} + \omega^2}{(R_1 + k_{\text{ex}})^2 + \omega^2} \quad (1)$$

where  $P_{\text{B}}$  is the mole fraction of the paramagnetic ions;  $k_{\text{ex}}$  is the chemical exchange rate;  $\omega$  is the chemical shift (in  $\text{rad s}^{-1}$ ) of the exchangeable proton on the agent;  $R_{2\text{ex}}$  is the transverse relaxation rate due to chemical exchange; and  $R_2$  is the transverse relaxation rate that only includes effects from energy exchange between dipoles.

Note that  $R_2 = 1/T_2$  and  $R_{2\text{ex}} = 1/T_{2\text{ex}}$ .  $R_2$  and  $R_{2\text{ex}}$  are known as relaxation rates, and  $T_2$  and  $T_{2\text{ex}}$  are known as relaxation time constants.

The Swift–Connick equation shows how  $T_{2\text{ex}}$  relaxation can be sensitive to environmental biomarkers. For example, an increase in temperature typically increases a chemical exchange rate. If the chemical exchange rate is relatively slow (left side of the Swift–Connick plot in Figure 7A), then heating the tissue will increase the  $R_{2\text{ex}}$  relaxation rate. Conversely, if the chemical exchange rate is very fast (right side of the Swift–Connick plot in Figure 7A), then heat will decrease the  $R_{2\text{ex}}$  relaxation rate. Therefore, this example shows that the chemistry of the  $T_{2\text{ex}}$  agent should be optimized to provide a slower or faster exchange rate, so that the  $R_{2\text{ex}}$  dependence on a desired temperature range is single valued. Similarly, the Swift–Connick equation shows that the magnetic field strength of the MRI scanner affects the  $R_{2\text{ex}}$  rate because the magnetic field strength determines the chemical shift (Equation 2). Therefore,  $T_{2\text{ex}}$  agents have more utility at higher magnetic field strengths (Figure 7B). The dependence of  $T_{2\text{ex}}$  agents on magnetic field strength, temperature, and other conditions that affect the chemical exchange rate has contributed to the uncertainty about how these secret agents truly operate.

$$\omega = \gamma B_0 \quad (2)$$

where  $\gamma$  is the gyromagnetic ratio, a fundamental property of a proton and  $B_0$  is the magnetic field strength in units of Tesla (T).

### The first $T_{2\text{ex}}$ agents

The first applications of  $T_{2\text{ex}}$  relaxation in 1970 were designed to suppress the large signal of water to observe the smaller signals from biomolecules in biological MR samples. Examples of these agents include urea, ammonium chloride, paramagnetic ions, and metal complexes.<sup>70</sup> Further studies showed that the intensity of the water signal could be systematically controlled by adjusting parameters of various MR acquisition protocols.<sup>71–74</sup> However, using these  $T_{2\text{ex}}$  “water suppressors” as MRI contrast agents remained a secret until 1988.<sup>75</sup> Since that time, both paramagnetic and diamagnetic  $T_{2\text{ex}}$  agents have been developed for biomedical imaging.

### Paramagnetic $T_{2ex}$ agents

The bound water molecule in some types of Dy(III) macrocyclic chelates can have a chemical shift as high as 800 ppm.<sup>63</sup> These Dy(III) chelates have a chemical exchange rate of  $0.2 \times 10^6$ – $2.7 \times 10^8$  Hz. The agent with the best  $T_{2ex}$  effect has a chemical exchange rate of  $5.5 \times 10^6$  Hz, and 98% of the  $T^2$  relaxation was estimated to be derived from the  $T_{2ex}$  process (Figure 7C). Preliminary in vivo studies with this best Dy(III)-based  $T_{2ex}$  agent showed an impressive order-of-magnitude improvement in detection sensitivity relative to other tested Dy(III) agents.

Other lanthanide chelates have  $T_{2ex}$  relaxation properties that are a fraction observed with Dy(III) chelates. For example, the chemical shifts of labile protons in Eu(III) chelates are ~16 times smaller than the chemical shifts in Dy(III). The best reported Eu(III)-based  $T_{2ex}$  agent has a chemical exchange rate of  $3.6 \times 10^5$  Hz at 9.4 T magnetic field strength and yet only produces 4.4% of the  $T_{2ex}$  relaxation demonstrated by the best Dy(III)-based  $T_{2ex}$  agent (Figure 7D).<sup>76</sup>

$T_{2ex}$  agents can also be biomarker-responsive contrast agents.<sup>77</sup> As a seminal example, a Tm(III) macrocyclic chelate has a weak  $T_{2ex}$  relaxation effect due to the agents' chemical exchange rates that are <15,000 Hz (Figure 7E). After reacting with nitric oxide, the chemical exchange rate of the agent (possibly including a bound water molecule) becomes >140,000 Hz, which produces stronger  $T_{2ex}$  relaxation. The  $T_1$  relaxation time of the agent does not change after interacting with nitric oxide. Therefore, the  $T_2/T_1$  ratio can detect nitric oxide in a concentration-independent manner. Originally designed to be a CEST agent, this novel agent was unexpectedly discovered to be a secret agent, with a responsive  $T_{2ex}$  relaxation effect.

### Diamagnetic $T_{2ex}$ agents

Although lanthanide-based paramagnetic agents generate large chemical shifts that improve  $T_{2ex}$  relaxation, lanthanide metals have potential toxicity that limit the amount that may be administered in vivo, which limits detection sensitivity. For comparison, diamagnetic agents have smaller chemical shifts that generate less  $T_{2ex}$  relaxation, but their potentially low toxicity allows for greater amounts of the agent that may be administered, which may improve detection sensitivity. As an example, iopamidol is a FDA-approved contrast agent for X-ray imaging and CT scans, which can be administered at high ~900 mM concentrations in large ~200 mL volumes. This agent has a relatively low  $T_{2ex}$  relaxation per molecule, but the very high amount can generate an easily detectable  $T_{2ex}$  relaxation effect.<sup>75</sup> This unintended property of this CT agent qualifies this molecule as a secret agent for MRI studies.

Carbohydrates have also showed noticeable  $T_{2ex}$  relaxation due to proton exchange with bulk water. Computational stimulations and experimental studies of monosaccharides and homopolysaccharides have shown that water molecules hydrogen bonded to the hydroxyl groups of the carbohydrates account for this  $T_{2ex}$  relaxation effect.<sup>78</sup> As another example, glucose can generate  $T_{2ex}$  relaxation due to its relatively fast chemical exchange rate of 4,600 Hz, especially at higher magnetic field strengths. Glucose is a natural product that can

be administered orally or intravenously at high concentrations in biological systems with very low toxicological risk.<sup>62</sup> This high amount of administration was a key to performing in vivo preclinical imaging studies that detected exogenous glucose with T<sub>2</sub>-weighted MRI methods. The T<sub>2ex</sub> relaxation of glucose was unknown when glucose was approved by the FDA to be a therapeutic agent and, therefore, glucose could be considered to be a secret agent for molecular imaging.

In addition to carbohydrates, peptides and proteins may also be used as T<sub>2ex</sub> agents. Exchangeable protons on the side chains of amino acids have chemical exchange rates as high as 10,000 Hz and have been known to produce significant T<sub>2</sub> relaxation.<sup>79</sup> However, the T<sub>2ex</sub> relaxation properties of peptides and proteins have not been fully characterized, so that these biomolecules remain as secret agents.

### Future directions for T<sub>2ex</sub> contrast agents

T<sub>2ex</sub> agents show promise as having good detection sensitivity, especially for agents with large chemical shifts or agents that can be administered at high amounts. However, the best-reported T<sub>2ex</sub> agents to date are still at least an order-of-magnitude less sensitive than common T<sub>2</sub> agents. Optimizing the chemical exchange rate of an agent can improve T<sub>2ex</sub> relaxation that leads to greater detection sensitivity. Moreover, delivering a greater amount of agent via polymerization or encapsulation may improve the detection of a nanoscale agent, as previously discussed with CEST agents in this review. Future investigations are warranted to improve detection using these approaches.

The example of a T<sub>2ex</sub> agent that can detect nitric oxide shows the potential of this class of agents to detect important biomarkers of many biological processes and disease states. Importantly, the T<sub>1</sub> relaxation time does not change when the chemical exchange rate of the agent remains in a slow-to-intermediate regime of chemical exchange rates. Thus, the T<sub>2</sub>/T<sub>1</sub> ratio is more specific for detecting a biomarker that changes T<sub>2ex</sub> relaxation, by using the T<sub>1</sub> relaxation as an “internal control”.<sup>80</sup> This approach causes these secret agents to also become double agents by having two independent relaxation effects. This “double-secret agent” approach has not been exploited beyond the seminal example of the nitric oxide-responsive T<sub>2ex</sub> agent. Therefore, future research will hopefully develop this emerging field of MRI contrast agent for molecular imaging.

### References

1. Davies GL, Kramberger I, Davis JJ. Environmentally responsive MRI contrast agents. *Chem Commun.* 2013; 49:9704–9721.
2. Lauterbur PC, Dias MHM, Rudin AM. Augmentation of tissue water proton spin-lattice relaxation rates by in-vivo addition of paramagnetic ions. *Front Biol Energ.* 1978; 1:752–759.
3. Ali MM, Guanshu L, Tejas S, Flask CA, Pagel MD. Using two chemical exchange saturation transfer magnetic resonance imaging contrast agents for molecular imaging studies. *Acc Chem Res.* 2009; 42(7):915–924. [PubMed: 19514717]
4. Ward KM, Balaban RS. Determination of pH using water protons and chemical exchange dependent saturation transfer (CEST). *Magn Reson Med.* 2000; 44:799–802. [PubMed: 11064415]
5. Yang X, Yadav NN, Song X, et al. Tuning phenols with Intra-Molecular Bond Shifted HYdrogens (IM-SHY) as diaCEST MRI contrast agents. *Chem Eur J.* 2014; 20:15824–15832. [PubMed: 25302635]

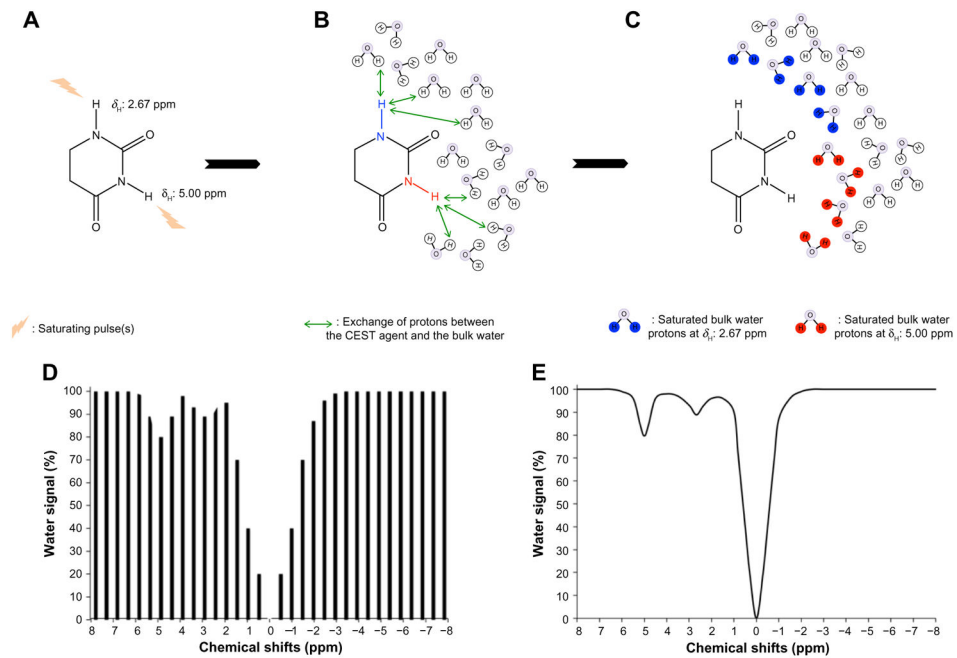
6. Yoo B, Pagel MD. A paraCEST MRI contrast agent to detect enzyme activity. *J Am Chem Soc.* 2006; 128:14032–14033. [PubMed: 17061878]
7. Suchý M, Ta R, Li AX, et al. A paramagnetic chemical exchange-based MRI probe metabolized by cathepsin D: design, synthesis and cellular uptake studies. *Org Biomol Chem.* 2010; 8:2560–2566. [PubMed: 20485791]
8. Yoo B, Sheth VR, Howison CM, et al. Detection of in vivo enzyme activity with catalyCEST MRI. *Magn Reson Med.* 2014; 71:1221–1230. [PubMed: 23640714]
9. Hingorani DV, Randtke EA, Pagel MD. A catalyCEST MRI contrast agent that detects the enzyme-catalyzed creation of a covalent bond. *J Am Chem Soc.* 2013; 135:6396–6398. [PubMed: 23601132]
10. Chauvin T, Durand P, Bernier M, et al. Detection of enzymatic activity by PARACEST MRI: a general approach to target a large variety of enzymes. *Angew Chem Int Ed Engl.* 2008; 47:4370–4372. [PubMed: 18454438]
11. Li Y, Sheth VR, Liu G, Pagel MD. A self-calibrating PARACEST MRI contrast agent that detects esterase enzyme activity. *Contrast Media Mol Imaging.* 2011; 6:219–228. [PubMed: 21861282]
12. Liu G, Liang Y, Bar-Shir A, et al. Monitoring enzyme activity using a diamagnetic chemical exchange saturation transfer magnetic resonance imaging contrast agent. *J Am Chem Soc.* 2011; 133:16326–16329. [PubMed: 21919523]
13. Jamin Y, Eykyn TR, Poon E, Springer CJ, Robinson SP. Detection of the prodrug-activating enzyme carboxypeptidase G2 activity with chemical exchange saturation transfer magnetic resonance. *Mol Imaging Biol.* 2014; 16:152–157. [PubMed: 23955100]
14. Wu Y, Carney CE, Denton M, et al. Polymeric paraCEST MRI contrast agents as potential reporters for gene therapy. *Org Biomol Chem.* 2010; 8:5333–5338. [PubMed: 20848030]
15. Nwe K, Andolina CM, Huang CH, Morrow JR. ParaCEST properties of a dinuclear neodymium(III) complex bound to DNA or carbonate. *Bioconjug Chem.* 2009; 20:1375–1382. [PubMed: 19555071]
16. Gilad AA, McMahan MT, Walczak P, et al. Artificial reporter gene providing MRI contrast based on proton exchange. *Nat Biotechnol.* 2007; 25:217–219. [PubMed: 17259977]
17. Minn I, Bar-Shir A, Yarlagadda K, et al. Tumor-specific expression and detection of a CEST reporter gene. *Magn Reson Med.* 2015; 74:544–549. [PubMed: 25919119]
18. Farrar CT, Buhman JS, Liu G, et al. Establishing the lysine-rich protein CEST reporter gene as a CEST MR imaging detector for oncolytic virotherapy. *Radiology.* 2015; 275:746–754. [PubMed: 25686366]
19. McMahan MT, Gilad AA, DeLiso MA, Cromer Berman SM, Bulte JWM, van Zijl PCM. New “multicolor” polypeptide diamagnetic chemical exchange saturation transfer (DIACEST) contrast agents for MRI. *Magn Reson Med.* 2008; 60:803–812. [PubMed: 18816830]
20. Bar-Shir A, Liu G, Chan KW, et al. Human protamine-1 as an MRI reporter gene based on chemical exchange. *ACS Chem Biol.* 2014; 9:134–138. [PubMed: 24138139]
21. Bar-Shir A, Liang Y, Chan KWY, Assaf A, Gilad AA, Bulte JWM. Supercharged green fluorescent proteins as bimodal reporter genes for CEST MRI and optical imaging. *Chem Commun.* 2015; 51:4869–4871.
22. Oskolkov N, Bar-Shir A, Chan KWY, et al. Biophysical characterization of human protamine-1 as a responsive CEST MR contrast agent. *ACS Macro Lett.* 2015; 4:34–38. [PubMed: 25642384]
23. Ren J, Trokowski R, Zhang S, Malloy CR, Sherry AD. Imaging the tissue distribution of glucose in livers using a paraCEST sensor. *Magn Reson Med.* 2008; 60:1047–1055. [PubMed: 18958853]
24. Aime S, Delli Castelli D, Fedeli F, Terreno E. A paramagnetic MRI-CEST agent responsive to lactate concentration. *J Am Chem Soc.* 2002; 124:9364–9365. [PubMed: 12167018]
25. Huang CH, Morrow JR. A paraCEST agent responsive to inner- and outer-sphere phosphate ester interactions for MRI applications. *J Am Chem Soc.* 2009; 131:4206–4207. [PubMed: 19317496]
26. Liu G, Li Y, Pagel MD. Design and characterization of a new irreversible responsive paraCEST MRI contrast agent that detects nitric oxide. *Magn Reson Med.* 2007; 58:1249–1256. [PubMed: 18046705]
27. Walker-Samuel S, Ramasawmy R, Torrealdea F, et al. In vivo imaging of glucose uptake and metabolism in tumors. *Nat Med.* 2013; 19(8):1067–1072. [PubMed: 23832090]



28. Chan K W Y, McMahon M T, Kato Y, et al. Natural D-glucose as a biodegradable MRI contrast agent for detecting cancer. *Magn Reson Med*. 2012; 68(6):1764–1773. [PubMed: 23074027]
29. Nasrallah F A, Pages G, Kuchel P W, Golay X, Chuang K H. Imaging brain deoxyglucose uptake and metabolism by glucoCEST MRI. *J Cereb Blood Flow Metab*. 2013; 33(8):1270–1278. [PubMed: 23673434]
30. Rivlin M, Horev J, Tsarfaty I, Navon G. Molecular imaging of tumors and metastases using chemical exchange saturation transfer (CEST) MRI. *Sci Rep*. 2013; 3:3045. [PubMed: 24157711]
31. Rivlin M, Tsarfaty I, Navon G. Functional molecular imaging of tumors by chemical exchange saturation transfer MRI of 3-O-methyl-D-glucose. *Magn Reson Med*. 2014; 72(5):1375–1380. [PubMed: 25236979]
32. Wang J, Hwang K, Fuller C, et al. SU-E-J-225: CEST imaging in head and neck cancer patients. *Med Phys*. 2015; 42(6):3317.
33. Trokowski R, Ren J, Kalman F K, Sherry A D. Selective sensing of zinc ions with a paraCEST contrast agent. *Angew Chem Int Ed Engl*. 2005; 44:6920–6923. [PubMed: 16206314]
34. Angelovski G, Chauvin T, Pohmann R, Logothetis N K, Tóth É. Calcium-responsive paramagnetic CEST agents. *Bioorg Med Chem*. 2011; 19:1097–1105. [PubMed: 20691598]
35. Tsitovich P B, Spornyak J A, Morrow J R. A redox-activated MRI contrast agent that switches between paramagnetic and diamagnetic states. *Angew Chem Int Ed Engl*. 2013; 52:13997–14000. [PubMed: 24222651]
36. Ratnakar S, Viswanathan J S, Kovacs Z, Jindal A K, Green K N, Sherry A D. Europium(III) DOTA-tetraamide complexes as redox-active MRI sensors. *J Am Chem Soc*. 2012; 134:5798–5800. [PubMed: 22420507]
37. Song B, Wu Y, Yu M, et al. A europium(III)-based paraCEST agent for sensing singlet oxygen by MRI. *Dalton Trans*. 2013; 14:8066–8069.
38. Zhang S, Malloy C R, Sherry A D. MRI thermometry based on paraCEST agents. *J Am Chem Soc*. 2005; 127:17572–17573. [PubMed: 16351064]
39. Li A X, Wojciechowski F, Suchy M, et al. A sensitive paraCEST contrast agent for temperature MRI: Eu<sup>3+</sup>-DOTAM-glycine(Gly)-phenylalanine(Phe). *Magn Reson Med*. 2008; 59:374–381. [PubMed: 18228602]
40. Stevens T K, Milneb M, Elmehrikib A A H, Suchý M, Bartha R, Hudson R H E. A DOTAM-based paraCEST agent favoring TSAP geometry for enhanced amide proton chemical shift dispersion and temperature sensitivity. *Contrast Media Mol Imaging*. 2013; 8:289–292. [PubMed: 23606433]
41. Zhang S, Michaudet L, Burgess S, Sherry A D. The amide protons of an ytterbium(III) dota tetraamide complex act as efficient antennae for transfer of magnetization to bulk water. *Angew Chem Int Ed Engl*. 2002; 41:1919–1921. [PubMed: 19750633]
42. Aime S, Delli Castelli D, Terreno E. Novel pH-reporter MRI contrast agents. *Angew Chem Int Ed Engl*. 2002; 114:4510–4512.
43. Sheth V R, Li Y, Chen L Q, Howison C M, Flask C A, Pagel M D. Measuring in vivo tumor pH with CEST-FISP MRI. *Magn Reson Med*. 2012; 67:760–768. [PubMed: 22028287]
44. Delli Castelli D, Terreno E, Aime S. YbIII-HPDO3A: a dual pH- and temperature-responsive CEST agent. *Angew Chem Int Ed Engl*. 2011; 50:1798–1800. [PubMed: 21328642]
45. Dorazio S J, Olatunde A O, Spornyak J A, Morrow J R. CoCEST: cobalt(II) amide-appended paraCEST MRI contrast agents. *Chem Commun*. 2013; 49:10025–10027.
46. Longo D L, Busato A, Lanzardo S, Antico F, Aime S. Imaging the pH evolution of an acute kidney injury model by means of iopamidol, a MRI-CEST pH-responsive contrast agent. *Magn Reson Med*. 2013; 70(3):859–864. [PubMed: 23059893]
47. Chen L Q, Randtke E A, Jones K M, Moon B F, Howison C H, Pagel M D. Evaluations of tumor acidosis within in vivo tumor models using parametric maps generated with acidoCEST MRI. *Mol Imaging Biol*. 2015; 17(4):488–496. [PubMed: 25622809]
48. Chen L Q, Howison C M, Spier C, et al. Assessment of carbonic anhydrase IX expression and extracellular pH in B-cell lymphoma cell line models. *Leuk Lymphoma*. 2015; 56(5):1432–1439. [PubMed: 25130478]

49. Melkus G, Grabau M, Karampinos DC, Majumdar S. Chemical exchange saturation transfer effect of glycosaminoglycan in the intervertebral disc. *Magn Reson Med*. 2014; 71:1743–1749. [PubMed: 23818244]
50. Longo DL, Sun PZ, Consolino L, Michelotti FM, Uggeri F, Aime S. A general MRI-CEST ratiometric approach for pH imaging: demonstration of in vivo pH mapping with iobitridol. *J Am Chem Soc*. 2014; 136:14333–14336. [PubMed: 25238643]
51. McVicar N, Li AX, Suchý M, Hudson RHE, Menon RS, Bartha R. Simultaneous in vivo pH and temperature mapping using a PARACEST-MRI contrast agent. *Magn Reson Med*. 2013; 70:1016–1025. [PubMed: 23165779]
52. Wu Y, Soesbe TC, Kiefer GE, Zhao P, Sherry AD. A responsive europium(III) chelate that provides a direct readout of pH by MRI. *J Am Chem Soc*. 2010; 132:14002–14003. [PubMed: 20853833]
53. Wu Y, Zhou Y, Ouari O, et al. Polymeric paraCEST agents for enhancing MRI contrast sensitivity. *J Am Chem Soc*. 2008; 130:13854–13855. [PubMed: 18817395]
54. Pikkemaat JA, Wegh RT, Lamerichs R, et al. Dendritic paraCEST contrast agents for magnetic resonance imaging. *Contrast Media Mol Imaging*. 2007; 2:229–239. [PubMed: 17937448]
55. Winter PM, Cai K, Chen J, et al. Targeted paraCEST nanoparticle contrast agent for the detection of fibrin. *Magn Reson Med*. 2006; 56:1384–1388. [PubMed: 17089356]
56. Aime S, Delli Castelli D, Terreno E. Highly sensitive MRI chemical exchange saturation transfer agents using liposomes. *Angew Chem*. 2005; 117:5649–5651.
57. Aime S, Delli Castelli D, Terreno E. Supramolecular adducts between poly-l-arginine and [TmIII dotp]: a route to sensitivity-enhanced magnetic resonance imaging-chemical exchange saturation transfer agents. *Angew Chem Int Ed Engl*. 2003; 42:4527–4529. [PubMed: 14520757]
58. Chan KWY, Bulte JWM, McMahon MT. Diamagnetic chemical exchange saturation transfer (diaCEST) liposomes: physicochemical properties and imaging applications. *Nanomed Nanobiotech*. 2014; 6(1):111–124.
59. Snoussi K, Bulte JWM, Guéron M, van Zijl PCM. Sensitive CEST agents based on nucleic acid imino proton exchange: detection of poly(rU) and of a dendrimer-poly(rU) model for nucleic acid delivery and pharmacology. *Magn Reson Med*. 2003; 49(6):998–1005. [PubMed: 12768576]
60. Kuo PH, Kanal E, Abu-Alfa AK, Cowper SE. Gadolinium-based MR contrast agents and nephrogenic systemic fibrosis. *Radiology*. 2007; 242:647–649. [PubMed: 17213364]
61. Dorazio SJ, Tsitovich PB, Sifers KE, Spornyak JA, Morrow JR. Iron(II) paraCEST MRI contrast agents. *J Am Chem Soc*. 2011; 133:14154–14156. [PubMed: 21838276]
62. Yadav NN, Xu J, Bar-Shir A, et al. Natural D-glucose as a biodegradable MRI relaxation agent. *Magn Reson Med*. 2014; 72:823–828. [PubMed: 24975029]
63. Soesbe TC, Ratnakar SJ, Milne M, et al. Maximizing T<sub>2</sub>-exchange in Dy<sup>3+</sup>DOTA-(amide)<sub>x</sub> chelates: fine-tuning the water molecule exchange rate for enhanced T<sub>2</sub> contrast in MRI. *Magn Reson Med*. 2014; 71:1179–1185. [PubMed: 24390729]
64. Sherry AD, Wu Y. The importance of water exchange rates in the design of responsive agents for MRI. *Curr Opin Chem Biol*. 2013; 17(2):167–174. [PubMed: 23333571]
65. Bloch F. Nuclear induction. *Phys Rev*. 1946; 70:460–474.
66. McConnell HM. Reaction rates by nuclear magnetic resonance. *J Chem Phys*. 1956; 28:430–431.
67. Leigh JS Jr. Relaxation times in systems with chemical exchange: some exact solution. *J Magn Reson*. 1971; 4:308–311.
68. Carver JP, Richards RE. A general two-site solution for the chemical exchange produced dependence of T<sub>2</sub> upon the Carr-Purcell pulse separation. *J Magn Reson*. 1972; 6:89–105.
69. Swift TJ, Connick RE. NMR-relaxation mechanisms of O<sup>17</sup> in aqueous solutions of paramagnetic cations and the lifetime of water molecules in the first coordination sphere. *J Chem Phys*. 1962; 37(2):307–320.
70. Vold RL, Daniel ES, Chan SO. Magnetic resonance measurements of proton exchange in aqueous urea. *J Am Chem Soc*. 1970; 92(23):6771–6776.
71. Bryant RG, Eads TM. Solvent peak suppression in high resolution NMR. *J Magn Reson*. 1985; 64(2):312–315.

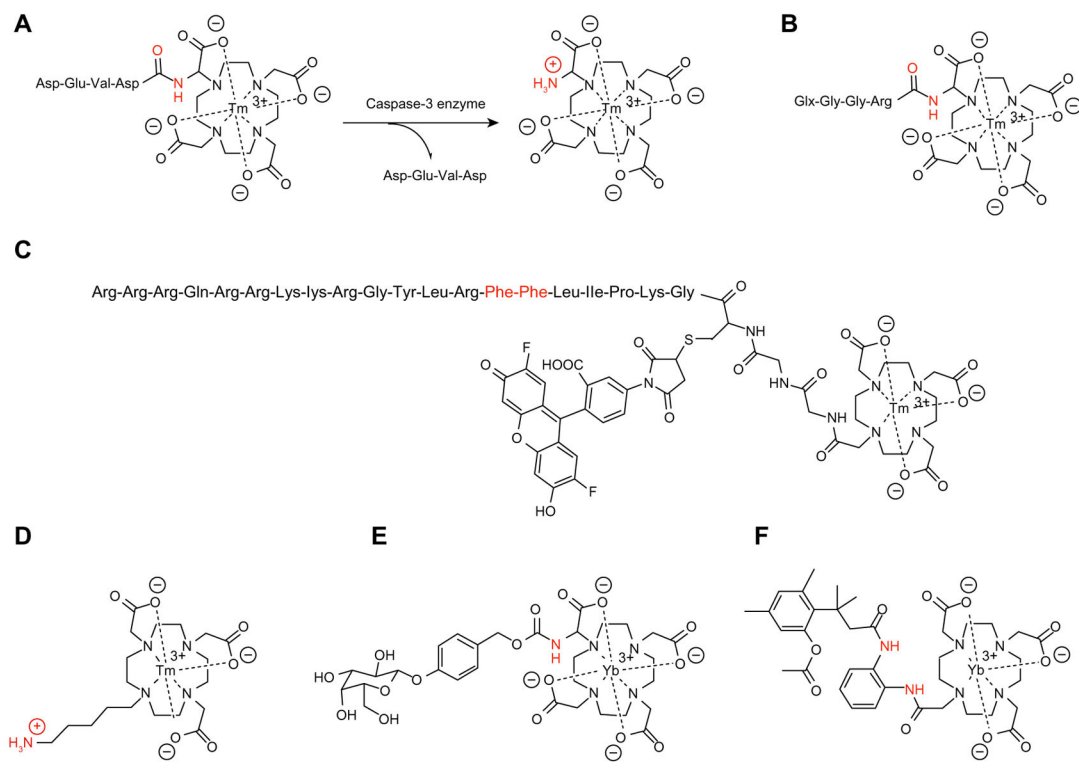
72. Granot J, Fiat D. Effect of chemical exchange on the transverse relaxation rate of nuclei in solution containing paramagnetic ions. *J Magn Reson.* 1974; 15(3):540–548.
73. Rabenstein DL, Fan S, Nakashima TT. Attenuation of the water resonance in Fourier transform  $^1\text{H}$  NMR spectra of aqueous solutions by spin-spin relaxation. *J Magn Reson.* 1985; 64(3):541–546.
74. Connor S, Nicholson JK. Chemical-exchange and paramagnetic  $T_2$  relaxation agents for water suppression in spin-echo proton nuclear magnetic resonance spectroscopy of biological fluids. *Anal Chem.* 1987; 59:2885–2891. [PubMed: 3434814]
75. Aime S, Nano R, Grandi M. A new class of contrast agents for magnetic resonance imaging based on selective reduction of water- $T_2$  by chemical exchange. *Invest Radiol.* 1988; 23:S267–S270. [PubMed: 3198360]
76. Soesbe TC, Merritt ME, Green KN, Rojas-Quijano FA, Sherry AD.  $T_2$  exchange agents: a new class of paramagnetic MRI contrast agent that shortens water  $T_2$  by chemical exchange rather than relaxation. *Magn Reson Med.* 2011; 66:1697–1703. [PubMed: 21608031]
77. Daryaei, I.; Pagel, MD. New type of responsive MRI contrast agent that modulates  $T_{2ex}$  relaxation: detection of nitric oxide. In: Allen, M.; Caravan, P.; Pierre, V., editors. *Proceedings of American Chemical Society.* Dallas TX: ACS Publications; 2014. p. 498
78. Hills BP, Cano C, Belton PS. Proton NMR relaxation studies of aqueous polysaccharide systems. *Macromolecules.* 1991; 24:2944–2950.
79. Liepinsh E, Otting G. Proton exchange rates from amino acid side chains – implications for image contrast. *Magn Reson Med.* 1996; 35(1):30–42. [PubMed: 8771020]
80. Aime S, Fedeli F, Sanino A, Terreno E. A  $R_2/R_1$  ratiometric procedure for a concentration-independent, pH-responsive, Gd(III)-based MRI agent. *J Am Chem Soc.* 2006; 128:11326–11327. [PubMed: 16939235]

**Figure 1.**

The mechanism of chemical exchange saturation transfer (CEST).

**Notes:** (A) Exchangeable protons are saturated with a radiofrequency pulse. (B) Saturated protons are exchanged between the CEST agents and the bulk water. (C) The bulk water loses part of its net MR signal due to the exchange of saturated protons. (D) Water signals are collected with a range of radiofrequencies. Direct saturation of bulk water is set as the reference (0 ppm). (E) Connecting the signals of bulk water generates a Z-spectrum.

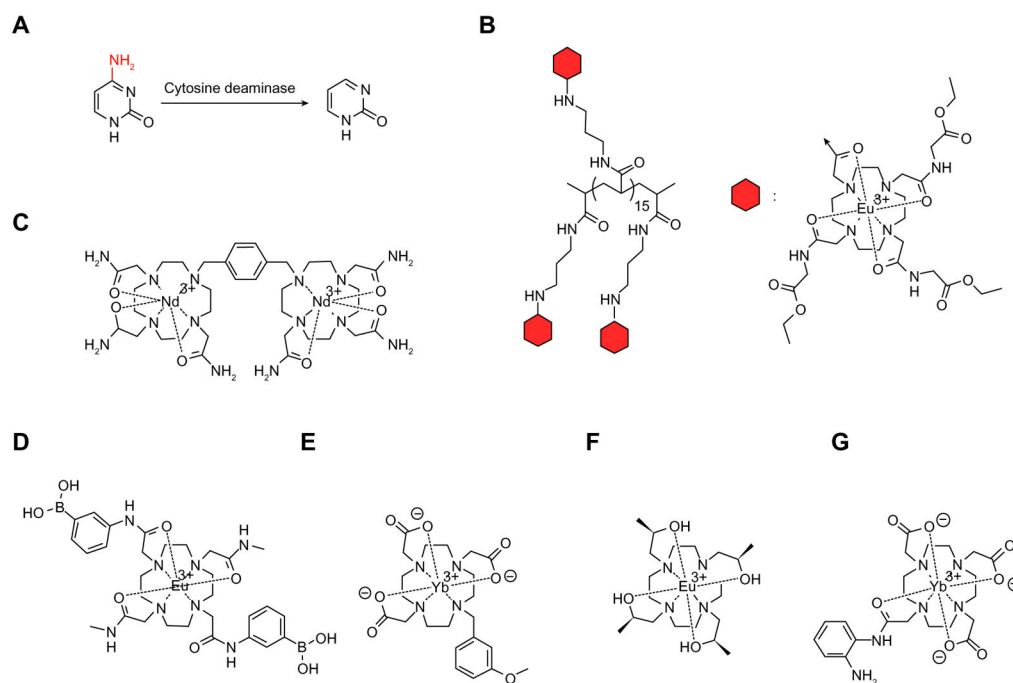
**Abbreviation:** MR, magnetic resonance.



**Figure 2.**  
ParaCEST agents that detect enzyme activity.

**Notes:** Agents have been designed that detect (A) caspase-3, (B) urokinase plasminogen activator, (C) cathepsin D, (D) transglutaminase, (E)  $\beta$ -galactosidase, and (F) esterase.

**Abbreviation:** ParaCEST, paramagnetic chemical exchange saturation transfer.

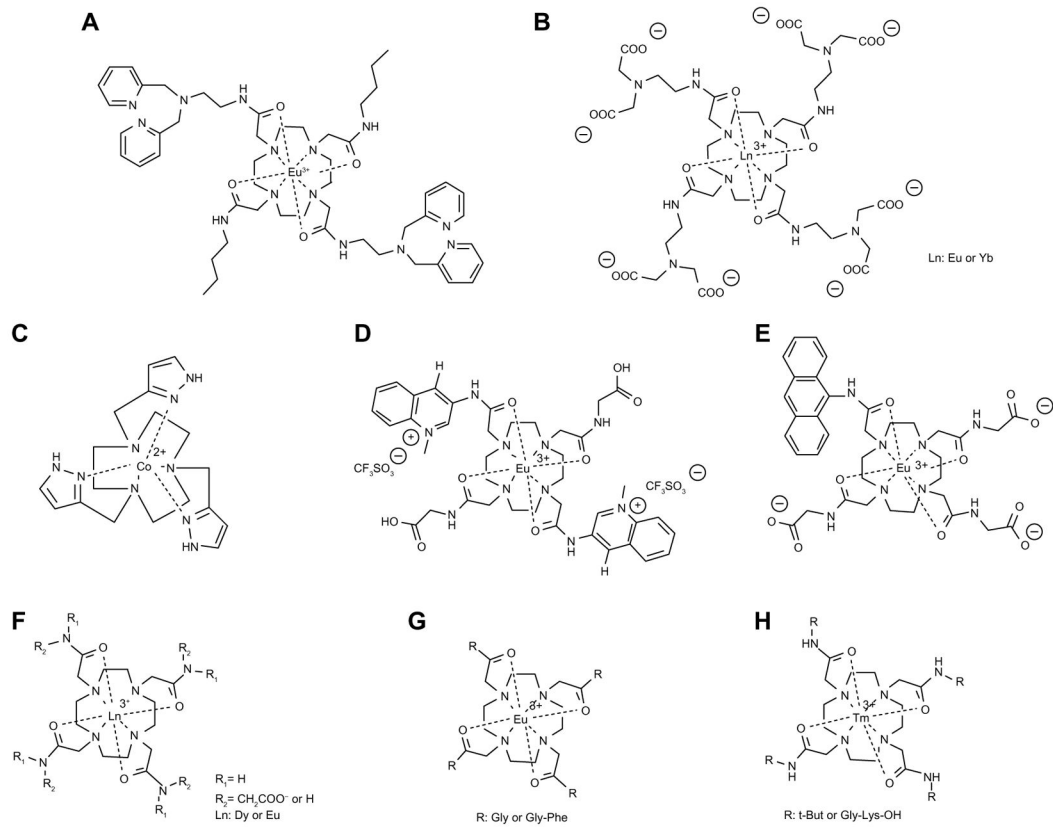


**Figure 3.**  
Responsive CEST agents.

**Notes:** (A) Deamination of cytosine by deaminase enzyme. Other agents can detect (B and C) DNA, (D) glucose, (E) lactate, (F) methyl phosphate, and (G) nitric oxide.

**Abbreviation:** CEST, chemical exchange saturation transfer.

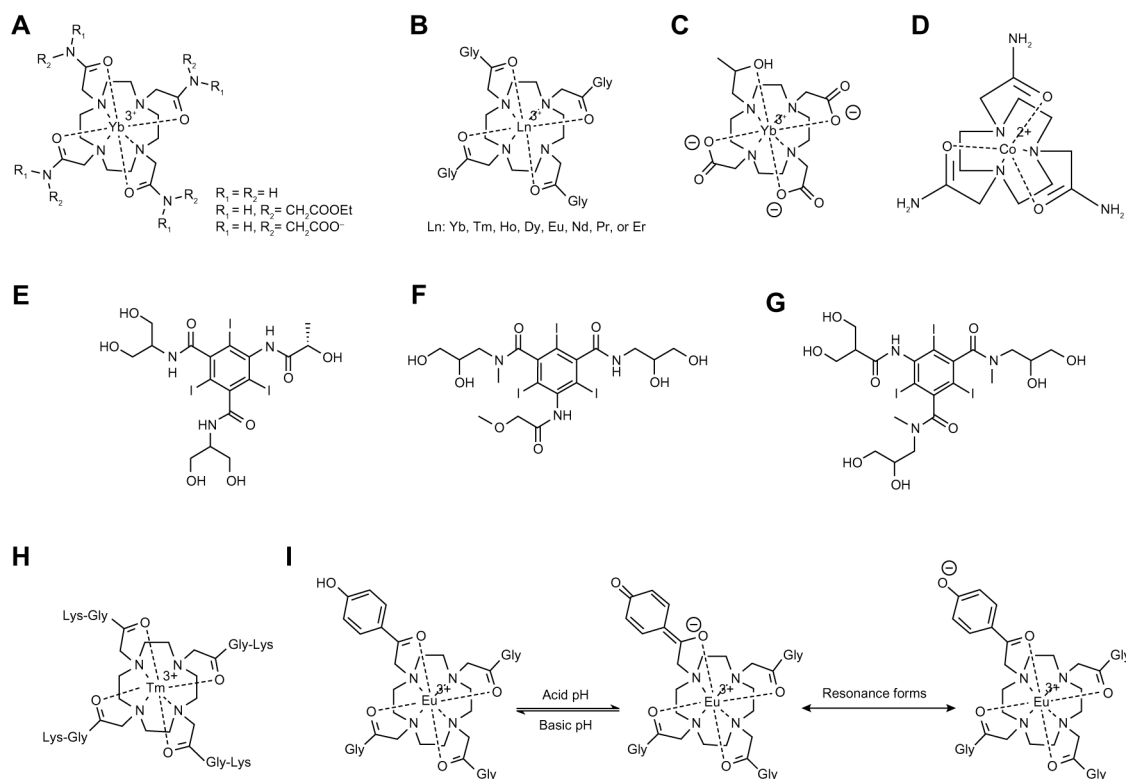


**Figure 4.**

ParaCEST agents that detect ions, redox state, and temperature.

**Notes:** Agents have been designed that detect **(A)**  $\text{Zn}^{2+}$ , **(B)**  $\text{Ca}^{2+}$ , and **(C–E)** redox conditions. **(F–H)** Other agents can measure temperature.

**Abbreviation:** ParaCEST, paramagnetic chemical exchange saturation transfer.

**Figure 5.**

CEST agents that measure pH include (A) Yb-DOTAM-Gly-X, (B) Ln-DOTAM-Gly, (C) Yb(III)-HPDO3A, (D) Co(II)-complex, (E) iopamidol, (F) iopromide, (G) iobitridol, (H) and Tm-DOTAM-Gly-Lys. (I) Deprotonation of a Eu(III) complex changes the coordination around the  $Eu^{3+}$  ion, which changes the CEST effect of this agent.

**Abbreviation:** CEST, chemical exchange saturation transfer.

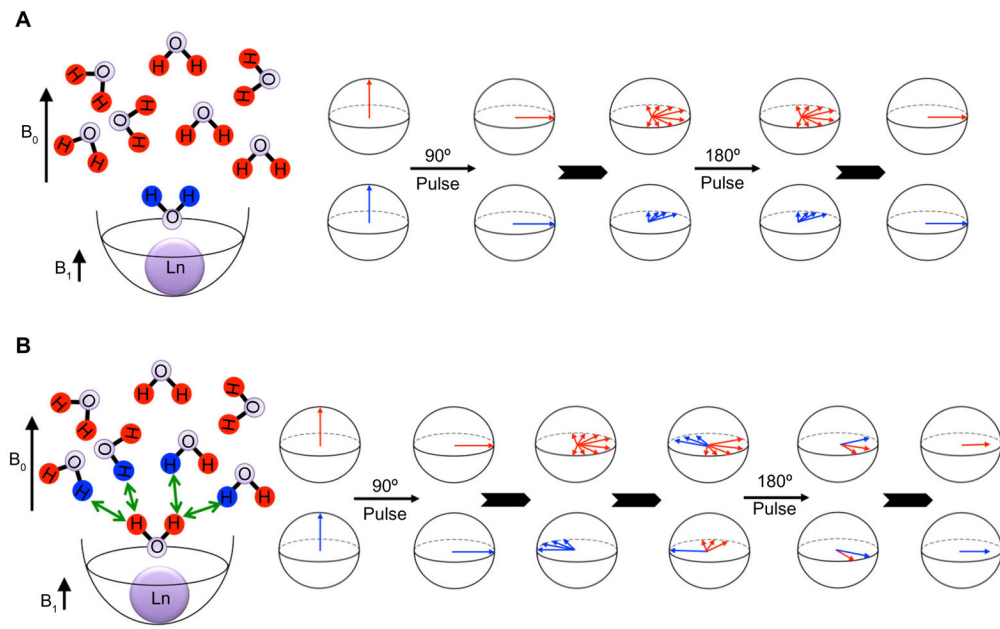


**Figure 6.**

The mechanism of the  $T_{2ex}$  process.

**Notes:** (A)  $T_2$  is measured by rotating the net magnetization into the transverse plane by an excitation pulse, then components of the net magnetization evolve to defocus, and then a 180° pulse causes these components to refocus. (B) The chemical exchange of protons with different phases causes cancellation of net magnetization, creating a shorter  $T_2$  relaxation time constant for the bulk water due to  $T_{2ex}$ .

**Abbreviation:**  $T_{2ex}$ ,  $T_2$  exchange.

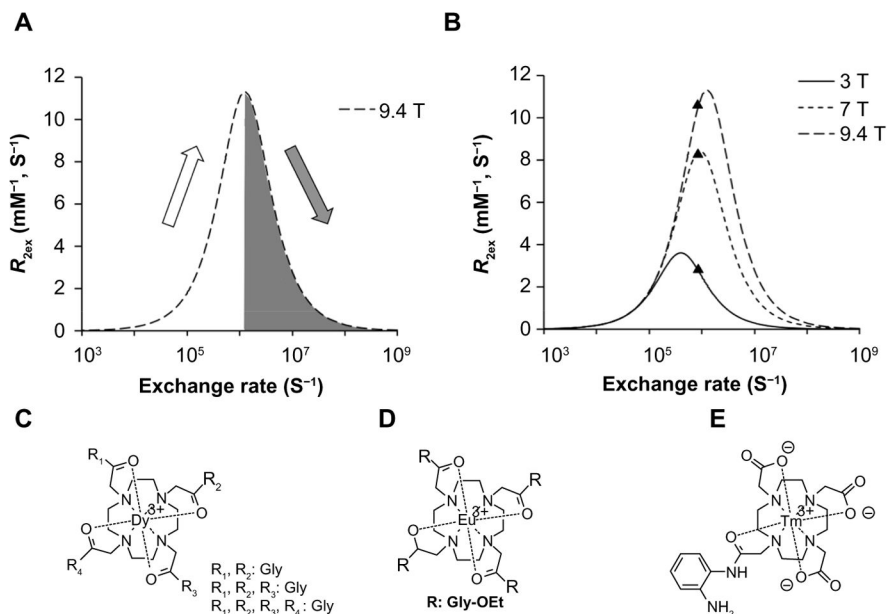


**Figure 7.**

The dependence of  $T_{2ex}$  on environmental conditions.

**Notes:** (A) An increase in temperature increases relaxivities on the rising side of Swift–Connick plot (shown by the white arrow), while an increase in temperature decreases relaxivities on the falling side of the Swift–Connick plot (shown by the gray arrow). (B) Triangles show relaxivities due to exchange of a proton with the same chemical shift and chemical exchange rate in three different magnetic fields. The chemical structures of (C) Dy-DOTAM-(Gly)<sub>x</sub> complexes, (D) Eu(III) complexes, and (E) Tm-DO3A-oAA show similar features that lead to  $T_{2ex}$  relaxation.

**Abbreviation:**  $T_{2ex}$ ,  $T_2$  exchange.